

# Spherically Imploding Plasma Liners as a Standoff Driver for Magnetoinertial Fusion

S. C. Hsu, T. J. Awe, S. Brockington, A. Case, J. T. Cassibry, G. Kagan, S. J. Messer, M. Stanic, X. Tang, D. R. Welch, and F. D. Witherspoon

(Invited Paper)

**Abstract**—Spherically imploding plasma liners formed by merging an array of high Mach number plasma jets are a proposed standoff driver for magnetoinertial fusion (MIF). This paper gives an updated concept-level overview of plasma liner MIF, including advanced notions such as standoff methods for forming and magnetizing the fuel target and liner shaping to optimize dwell time. Results from related 1-D radiation-hydrodynamic simulations of targetless plasma liner implosions are summarized along with new analysis on the efficiency of conversion of the initial liner kinetic energy to stagnation thermal energy. The plasma liner experiment (PLX), a multi-institutional collaboration led by the Los Alamos National Laboratory, plans to explore the feasibility of forming spherically imploding plasma liners via 30 merging plasma jets. In the near term, with modest pulsed power stored energy of  $\lesssim 1.5$  MJ, PLX is focusing on the generation of centimeter-, microsecond-, and megabar-scale plasmas for the fundamental study of high energy density laboratory plasmas. In the longer term, PLX can enable a research and development path to plasma liner MIF ultimately requiring compressing magnetized fusion fuel to  $\gtrsim 100$  Mbar.

**Index Terms**—Fusion reactors, plasmas.

## I. INTRODUCTION

**T**HIS paper describes the concept of spherically imploding plasma liners as a standoff driver for magnetoinertial fusion (MIF) [1], [2] as well as a nascent research program [3] that can ultimately assess and demonstrate the concept's feasi-

bility. The imploding spherical plasma liners are to be formed by an array of merging plasma jets launched by electromagnetic plasma accelerators from the periphery of a large spherical vacuum chamber. Once formed, the spherical plasma liner implodes toward the origin (carrying the initial momentum of the plasma jets). In principle, at least two distinct MIF approaches might be enabled by this scheme: 1) plasma liner compression of a preformed magnetized target plasma, similar to magnetized target fusion (MTF) concepts [4]–[7], and 2) the imploding (“composite”) plasma liner itself carries the main fusion fuel at its leading edge, and the fuel is magnetized prior to compression. In either case, the imploding liner may be a composite liner carrying a dense deuterium–tritium (D-T) “afterburner” layer in front to provide additional fuel that may burn and amplify the total fusion yield if it can be heated to the necessary conditions by the  $\alpha$  particles and radiation from the compressed burning main target fuel. For the first approach described above, it is envisioned that a subset of plasma jets (fired first) would carry the main D-T fuel, which would get magnetized prior to compression, whereas the remainder of the jets (fired slightly later) carry the composite liner material consisting of the D-T afterburner layer in front and a heavier inert species in the rear. Much further research is required to develop credible implementations of either approach and to determine which approach is more favorable for fusion energy.

The spherically imploding plasma liner concept for MIF was first proposed by Thio et al. [8], [9] in the late 1990s, inspired by Thio’s extensive work in the area of electromagnetic plasma accelerators coupled with a desire for an MIF standoff driver that would avoid repetitive destruction of solid liners and transmission lines. Analytic calculations [8] and 3-D hydrodynamic simulations [10] were performed to provide the first assessments of the plasma jet parameters required to form a plasma liner and compress a magnetized target plasma to fusion conditions. It was realized that electromagnetic plasma accelerators at the time could not achieve the required combination of mass, density, and velocity (described in Section III-A). Consequently, Thio carried out research [11] that led to a theoretical understanding, supported by numerical modeling [12], of how to improve on existing electromagnetic plasma accelerators to achieve the required jet parameters. The key insights were to use a preionized plasma rather than a neutral gas fill in the accelerator stage and to prevent blowby instability [12] by

Manuscript received September 13, 2011; revised December 5, 2011; accepted January 28, 2012. Date of publication March 12, 2012; date of current version May 9, 2012. This work was supported in part by the Office of Fusion Energy Sciences of the U.S. Department of Energy under Contract DE-AC52-06NA25396, Contract DE-FG02-05ER54810, Contract DE-FG02-05ER54835, and Contract DE-SC0003560, and in part by the Los Alamos National Laboratory Directed Research and Development (LDRD) Program.

S. C. Hsu is with the Physics Division, Los Alamos National Laboratory, Los Alamos, NM 87545 USA (e-mail: scotthsu@lanl.gov).

T. J. Awe was with the Physics Division, Los Alamos National Laboratory, Los Alamos, NM 87545 USA. He is currently with Sandia National Laboratories, Albuquerque, NM 87185 USA.

S. Brockington, A. Case, S. J. Messer, and F. D. Witherspoon are with HyperV Technologies Corporation, Chantilly, VA 20151 USA.

J. T. Cassibry and M. Stanic are with the Propulsion Research Center, University of Alabama in Huntsville, Huntsville, AL 35899 USA.

G. Kagan and X. Tang are with the Theoretical Division, Los Alamos National Laboratory, Los Alamos, NM 87545 USA.

D. R. Welch is with Voss Scientific, Albuquerque, NM 87108 USA.

Color versions of one or more of the figures in this paper are available online at <http://ieeexplore.ieee.org>.

Digital Object Identifier 10.1109/TPS.2012.2186829

shaping the accelerator electrodes, which allowed most of the plasma fill mass to get accelerated to high velocity.

In 2004, an experimental research program and HyperV Technologies Corp. were initiated to build and optimize electromagnetic plasma accelerators based on the new insights developed over the prior several years. Since then, HyperV has demonstrated steady advances and set records for the combination of jet mass, density, and velocity [13]. Their initial work focused on the larger coaxial guns with shaped electrodes [14], [15], as suggested by Thio's research. In the past few years, HyperV's focus has shifted (temporarily) to simpler more compact parallel plate "mini-railguns" that were originally intended only to ionize and inject the plasma prefill into the coaxial guns. However, it was realized that the mini-railguns, much simpler and less expensive than the coaxial guns, could achieve the combination of mass (few milligrams), ion density ( $10^{17} \text{ cm}^{-3}$ ), and velocity (50 km/s) required for subscale (and targetless) spherical plasma liner formation and the implosion experiments to be carried out on the plasma liner experiment (PLX) [3] at the Los Alamos National Laboratory (LANL). Thus, for reasons of cost and expediency, mini-railguns are receiving most of the present research attention, although it must be emphasized that the coaxial guns (and their further development) are needed for fusion energy relevant plasma liner implosions due to their projected ability to accelerate large masses (10–100 mg) to high velocities ( $\gtrsim 100 \text{ km/s}$ ), their potential for forming composite (layered) jets, and their lower impurity levels. There is also potential for other fusion energy [16] spin-off applications, such as tokamak refueling or edge localized mode pacing, for HyperV's plasma guns.

In 2008, a workshop [17] was held at LANL to ponder the next steps for developing the plasma liner MIF concept. Several studies, summarized in [17], suggested that this concept has promise both for reaching high energy density (HED) conditions and for MIF, but support for the concept was not unanimous among the attendees [18]. The workshop provided an update on the status of plasma gun development, showing that the gun technology was ready for a subscale plasma liner formation demonstration. In addition, included in the workshop were several presentations related to a code development effort to combine the electromagnetic particle-in-cell (PIC) capability of the Large Scale Plasma (LSP) simulation code [19] with Prism Computational Sciences' [20] advanced equation-of-state (EOS) and opacity models. Such a modeling capability is required to fully assess the plasma liner MIF concept, particularly with respect to modeling plasma jet formation and gun physics, as well the significant portions of the liner evolution where radiative and kinetic effects are important. Furthermore, such a code capability would benefit the entire field of HED laboratory plasma research. A large subset of the workshop attendees believed that much more research was warranted and needed to fully assess the potential of the concept. A team was assembled to formulate the present PLX research program aimed at exploring and demonstrating the feasibility of forming spherically imploding plasma liners via merging plasma jets to reach 1 Mbar of peak pressure upon stagnation. With a relatively modest investment, PLX promises near term assessment of the feasibility and quality of plasma liner formation via

merging plasma jets while establishing a unique experimental facility capable of forming centimeter-, microsecond-, and megabar-scale plasmas for HED scientific studies. PLX is also a logical first step toward a potential plasma liner MIF research and development program.

Construction of the PLX facility at LANL was completed in August 2011, and experimental physics campaigns on single-jet propagation and two-jet merging are now underway [3]. Thirty jet experiments to form and study converging plasma liners (without a magnetized target) expected to reach 1 Mbar of peak pressure are to begin in 2013 (subject to availability of funding). Radiation-hydrodynamic simulations [21] using the 1-D Lagrangian RAVEN code [22] have explored both PLX- and MIF-relevant liner parameter spaces (without a magnetized target) and established a physical picture of liner implosion, stagnation, and poststagnation dynamics. Ideal hydrodynamics simulations using the 3-D Smooth Particle Hydrodynamics Code (SPHC) [24] are being used to evaluate important issues of 30 jet implosions and peak pressure scaling with initial jet parameters [25]. The LSP code with EOS/opacity modeling capability is run using a two-fluid model (with collisions between ions and electrons modeled as drag terms in the fluid equations of motion) [26] to generate detailed predictions of jet propagation. For jet merging predictions, the LSP code is run using a collisional hybrid PIC model with kinetic ions and fluid electrons. Synthetic interferometry and spectroscopy data are generated from the simulation output, all of which will guide initial experiments and be compared directly with experimental data. Tech-X Corp.'s Nautilus code [27], a Eulerian two-fluid magnetohydrodynamics (MHD) code with EOS modeling, is also being used as an independent comparison with the LSP results. Detailed research results from the SPHC, LSP, and Nautilus codes will be reported in separate forthcoming papers. The PLX facility will also be used to study cosmically relevant collisionless shocks [28] generated by the head-on collision of two lower-density but higher-velocity plasma jets. The facility has the potential to become a unique experimental platform for scientific studies of many of the research areas recognized in the report on HED laboratory physics research needs [29].

The rest of this paper is organized as follows. Section II describes the key features of MIF. Section III provides a concept-level description of plasma liner MIF. Section IV summarizes recent 1-D radiation-hydrodynamic scaling studies of the PLX- and MIF-relevant parameter space of imploding spherical plasma liners (without a magnetized target), and Section V describes the PLX facility and research plan. The final section provides a summary.

## II. KEY FEATURES OF MIF

MIF [1], [2] is a class of pulsed fusion approaches that includes a strong magnetic field in the compressed fusion fuel. The key resultant physics effects of the magnetic field are that it reduces thermal conduction within and enhances fusion charged product heating of the compressed burning fuel. The primary benefits are a significant enlargement of the areal density ( $\rho r$ ) parameter space for ignition [2] and relaxed requirements on implosion velocity. Batch burn (as opposed to propagating

burn) ignition becomes possible at  $\rho r \lesssim 0.01 \text{ g/cm}^2$ , and  $Br$  rather than  $\rho r$  becomes the key figure of merit for fusion ignition [30]. In the  $\rho r \sim 0.01 \text{ g/cm}^2$  ignition regime, MIF exploits lower required implosion velocities (1–100 km/s), allowing the use of more economic efficient pulsed power drivers (compared to laser drivers) with up to 50% “wall-plug” efficiency [31], [32]. With such efficiencies, MIF energy gains as low as 20 could give a gain efficiency product of 10, which is the nominal requirement for a viable inertial fusion energy (IFE) concept. It is important to note that, unlike in pure inertial confinement fusion (ICF), where the inertial confinement is determined by the fuel  $\rho r \gtrsim 1 \text{ g/cm}^2$ , in MIF, the inertial confinement is provided by the liner  $\rho r$ , which is much higher than the fuel  $\rho r \sim 0.01 \text{ g/cm}^2$ . For plasma liner MIF, the aim is to achieve inertial confinement times approaching  $1 \mu\text{s}$ , potentially enabling fuel burn-up fractions of 5–10%.

A recent paper [33] has shown why the  $\rho r \sim 0.01 \text{ g/cm}^2$  MIF regime represents a “sweet spot” in thermonuclear fusion parameter space. Using physics first principles to identify the thermonuclear parameter space and taking into account plasma size, energy, and power, a model is developed that accurately predicts the order-of-magnitude capital cost of ITER ( $\sim$ US \$10B), NIF ( $\sim$ US \$1B), as well as pulsed power facilities such as Z or ATLAS ( $\sim$ US \$100M) that are suitable for an MIF breakeven demonstration attempt. Note that these costs are only for the fusion core/driver and do not include the substantial additional costs needed for an actual fusion reactor, such as for tritium breeding and steady-state or repetitive operation. There are plans in the near future to field a breakeven-class MIF scheme called MagLIF [34] on Z. A conclusion of Lindemuth’s paper is the following: given the seriousness of the world’s energy problem, a potentially lower-cost fusion development path such as MIF warrants more examination than it has received to date.

Other ongoing MIF research activities include the solid liner MTF collaboration [5] between LANL and the Air Force Research Laboratory at Kirtland Air Force Base, the aforementioned MagLIF on Z [34], magnetized laser-driven implosions on the OMEGA laser at the University of Rochester (where enhanced neutron yields were observed recently in laser driven implosions of capsules with a seed magnetic field) [35], magnetokinetic and plasma liner compression of field-reversed configurations [7], [36], and piston-driven liquid liner compression of a compact toroid at General Fusion [6]. In addition, there is interest [37] in plasma liner MIF in Russia, which has a long history in MIF [38]. Most MIF concepts are based on cylindrical geometry and compression. The spherical compression of plasma liner MIF means that the fuel temperature increases more strongly as  $R^{-2}$ , eliminating the need to preheat the fuel to several hundred electronvolts as in cylindrical MIF concepts.

### III. CONCEPTUAL DESCRIPTION OF PLASMA LINER MIF

This section gives a concept-level description, as shown schematically in Fig. 1, of plasma liner MIF in sequential steps and the scientific key issues associated with each step. Advanced features such as the use of a dense D-T fuel afterburner layer in the liner (to amplify energy gain) and liner profile shaping (to optimize the burn time) are also discussed.

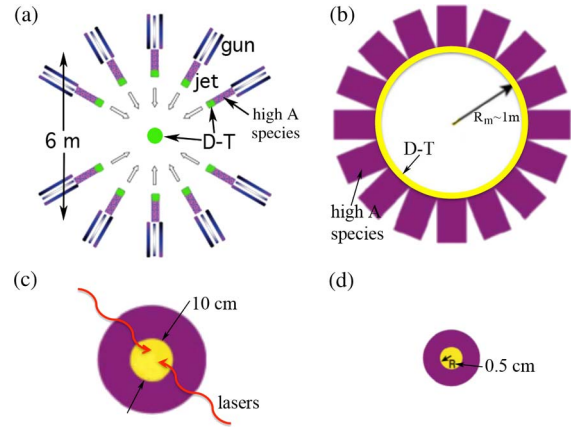


Fig. 1. Cross-sectional view of the composite plasma liner MIF concept. (a) High Mach number plasma jets (length  $\sim 10 \text{ cm}$ ) with D-T in the front and a heavy pusher element in the back (e.g., Xe) are launched from the periphery of a  $\sim 6\text{-m}$  radius spherical vacuum chamber. The D-T at the front of the jet might contain a lower-density hotter-fuel layer surrounded by a higher-density colder afterburner layer for the targetless version of the concept. In (a), a preformed target (formed by a subset of plasma jets fired earlier) is shown. (b) The jets merge at the merging radius  $R_m \sim 1 \text{ m}$ , forming an imploding plasma liner that further converges toward the origin. The preformed target is not shown here. (c) Prior to stagnation, lasers are launched (red) for beat wave current drive magnetization of the D-T fuel (D-T radius at this stage  $\sim 5 \text{ cm}$ ). (d) Stagnation and peak pressure are reached ( $R \sim 0.5 \text{ cm}$ ), followed by a precipitous drop of pressure and disassembly of the entire system when the outward going shock reaches the tail end of the incoming liner. Figures are not to scale, and subfigure (a) is adapted from [9].

The important question of achievable energy gain of plasma liner MIF is being studied using a 1-D Lagrangian hydrodynamic code [39]. These initial studies are idealized in that magnetic field effects are not treated self-consistently but are rather approximated by reducing or turning off thermal transport in the code, and  $\alpha$ -particle deposition is an adjustable parameter. In addition, these studies thus far have used only an ideal gas EOS and have neglected radiation losses. With these caveats in mind, preliminary (unoptimized) results [39] show energy gains around 10 with a 44-MJ plasma liner, with slightly less than half of the yield coming from the main D-T fuel layer and slightly more than half from the afterburner layer. The volume- and time-integrated yields were calculated based on the local density and temperature profiles. The initial conditions for this particular run are: 4.6 cm radius spherical D-T target with uniform  $n = 4.3 \times 10^{18} \text{ cm}^{-3}$ ,  $T = 90 \text{ eV}$ ,  $v = 45 \text{ km/s}$ , surrounded by a 0.136-cm-thick D-T afterburner with average  $n = 1.6 \times 10^{20} \text{ cm}^{-3}$ ,  $T = 2.4 \text{ eV}$ ,  $v = 39 \text{ km/s}$ , surrounded by a 3.5-cm-thick xenon liner with average  $n = 1.1 \times 10^{20} \text{ cm}^{-3}$ ,  $T = 1.4 \text{ eV}$ ,  $v = 45 \text{ km/s}$ . The 14.1-MeV neutron plus 3.5-MeV  $\alpha$ -particle fusion yield is 447 MJ. Detailed results from these and related studies will be reported in a separate forthcoming paper. Physics and engineering optimizations could further improve the gain values, whereas inclusion of more self-consistent physics in the simulations such as radiation transport in the D-T fuel and 3-D effects could reduce the gain. Therefore, much more work is needed with a state-of-the-art 3-D radiation-MHD code such as HYDRA [40] or GORGON [41] to explore further the viability of plasma liner MIF for fusion energy and to optimize the required initial conditions prior to compression.



TABLE I  
SUMMARY OF ACHIEVED AND REQUIRED PLASMA JET PARAMETERS.  
NOTE THAT COAXIAL GUNS HAVE ONLY BEEN TESTED UP TO  
HUNDREDS OF KILOAMPERES THUS FAR, AND THAT SEVERAL  
MEGAAMPERES ARE REQUIRED TO APPROACH THE  
FUSION-RELEVANT JET PARAMETERS

jet parameter	railgun achieved	coaxial gun achieved	PLX requirement	fusion requirement
density ( $\text{cm}^{-3}$ )	$10^{17}$	$10^{15}$	$10^{17}$	$10^{18}$
mass (mg)	5	0.3	8	10–100
velocity (km/s)	> 40	90	50	50–100
liner species	Ar	$\text{C}_2\text{H}_4$	Ar, Xe	Xe

#### A. Plasma Jets Launched From Periphery of Vacuum Chamber

Plasma jets of the required species, total mass, density, and velocity (see Table I) are formed and launched from electromagnetic plasma accelerators mounted at the surface of a large vacuum chamber (with a radius of several meters). One approach is to use a subset of jets (fired first) to form a D-T target that needs to get magnetized (see Section III-C) by the time it reaches the origin, with the remainder of the jets (fired slightly later) carrying the afterburner D-T layer and the heavy pusher layer (consisting of argon, krypton, or xenon). The second approach is for the jets to be fired all at once, carrying the main D-T fuel, D-T afterburner, and pusher layers. In either case, the main D-T fuel eventually needs to become compressed and magnetized to a level (order 100 T) required for fusion burn (see Section III-C regarding magnetization), and the afterburner D-T layer (if present) is intended to provide a buffer between the main D-T fuel and the outer pusher material against the cooling effects of the mix. The afterburner is also intended to supply additional fuel that could also burn to amplify the energy gain. The heavy pusher layer is envisioned to fulfill four separate physics functions: 1) it provides higher mass for a given (gun-limited) number density to provide the needed initial jet kinetic energy at more modest velocities; 2) the heavier element with both higher  $m_i$  and lower effective  $\gamma$  enhances the jet Mach number  $M \sim (m_i/\gamma)^{1/2}$ , which is a key figure of merit for reaching high liner stagnation pressures  $\sim M^{3/2}$  [21]; 3) the jet/liner is kept cool and compressible during propagation/convergence due to the effective atomic line radiation and cooling associated with having many bound electrons; and 4) upon stagnation and burn, the heavy pusher element helps to trap the radiation from the burning core, thus enhancing the energy confinement time.

The number of jets  $N$  needed is determined by several competing and interdependent requirements. A higher  $N$  (up to hundreds) is favored for point designs with larger  $R_m$ , for potentially better liner symmetry and uniformity, to minimize the merging angle (and hence shock heating, see Section III-B1) between adjacent jets and to reduce the required size, energy, and mass of each jet for a given  $R_m$ . A lower  $N$  (several dozen) is favored for point designs with smaller  $R_m$ , for better compatibility with liquid first wall reactor implementations (see Section III-E), and for simpler facility engineering and maintenance.

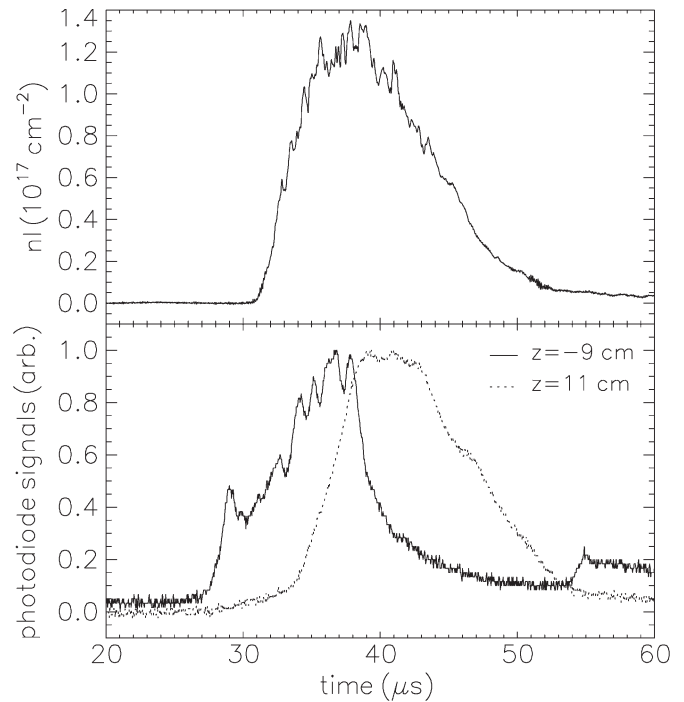


Fig. 2. (Top) Interferometer data of sight-line-integrated electron density ( $nl$ ) of a plasma jet, transverse to its direction of propagation, 1 cm outside the end of the 5-cm diameter plasma gun nozzle. (Bottom) Photodiode intensity (normalized) signals at two different axial distances from the end of the gun nozzle.

Claims that very high initial jet Mach numbers  $M > 60$  are needed [18], [42] were based on the requirement of minimizing density degradation due to jet thermal expansion during jet propagation from the chamber wall to  $R_m$ . However, those claims did not take into account that the jet temperature falls and  $M$  increases during propagation due to adiabatic expansion and radiative cooling, with the latter expected to be dominant in the case of a high atomic number liner species. Recent numerical modeling [21], [43], [44] has shown that argon jets with initial temperatures in the 3–10 eV range quickly cool to less than 1 eV well before the jet reaches  $R_m$ . This means that it is possible to form and accelerate a highly ionized plasma jet with modest  $M$  and then subsequently achieve the desirable situation, where  $M$  doubles by the time the jet reaches  $R_m$  to a value needed to ultimately reach fusion-relevant liner stagnation pressures. Radiative cooling is not as effective in the D-T fuel layers, although it still enjoys cooling in transit via adiabatic expansion. More research is needed to arrive at optimized composite jet initial parameters and profiles and, for that matter, the ability to form the required composite jets in the laboratory. Another ongoing area of research is determining the effects of jet density and temperature profiles on jet propagation, merging, peak liner stagnation pressure, and dwell time.

A PLX prototype railgun has generated plasma jets of more than 5-mg argon mass (measured by a ballistic pendulum) exceeding 25 km/s (Fig. 2) at around 38-kV gun voltage and 380-kA gun current [13]. By increasing the railgun current to 500–600 kA as planned, the PLX design goal of 8 mg at 50 km/s should be attainable. The data in Fig. 2 imply a peak jet electron density in the  $10^{17} \text{ cm}^{-3}$  range and a jet velocity exceeding 25 km/s. The jet velocity is estimated as follows: the photodiode

sightlines are separated by 20 cm, and the signal peaks are separated by about 4  $\mu\text{s}$ , implying a bulk jet speed of (20 cm)/(4  $\mu\text{s}$ ) > 25 km/s. Spectroscopy and time-of-flight data confirm a speed in the 25-km/s range for this shot. Jets exceeding 40 km/s based on photodiode array measurements have also been obtained [13], but density and mass measurements for those jets are still in progress. PLX plans to merge jets with a total kinetic energy for the 30 jets exceeding 300 kJ to achieve a peak stagnation pressure of around 1 Mbar. A fusion-relevant liner implosion would require higher jet mass/velocity and total liner energy (perhaps in the 30- to 50-MJ range) to reach peak pressures  $\gtrsim 100$  Mbar [21], [39] (see Table I). In general, higher plasma jet mass and velocity require higher gun current, which requires higher capacitive stored energy and charge voltage. While railguns are suitable for single-shot exploratory liner studies on PLX, coaxial guns operating at a few megaamperes and up to 100 kV will be needed for fusion-relevant liner implosions. For a pulse length of 1  $\mu\text{s}$ , this would translate to a few Coulombs per gun per shot, a challenging requirement for switching. A dedicated sustained coaxial gun development program to achieve fusion-relevant jet parameters would be required. Plasma gun and pulsed power issues for fusion-relevant repetitive operation are discussed in Section III-E.

### B. Jets Merge to Form Imploding Plasma Liner and Subsequent Liner Convergence

1) *Jet Merging*: At the merging radius  $R_m$ , the leading edges of the jets meet to form the leading edge of the imploding spherical plasma liner. Since the jets are supersonic, shocks may form even at oblique merging angles  $\theta > 2 \arcsin(1/M)$ , where  $\theta$  (in radians) is the angle between adjacent jets. Shock heating may defeat the beneficial cooling aspects discussed above, and too much shock heating will reduce the jet  $M$  and ultimately degrade the peak stagnation pressure. The shocks may also prove troublesome for maintaining the required liner symmetry and uniformity (see Section III-B2).

However, the picture is not so straightforward. The shocks are predicted to form in a pure fluid treatment of the problem described above. In reality, the ion collisional mean free path of the merging jets is less than but on the same order as the jet radius, and thus, some interpenetration of jet ions is expected. Whether a shock would even form is an open question. An accurate treatment of this problem requires two-fluid or hybrid PIC models because, due to the high ion directed velocity (>50 km/s) and cold electron temperature (< few eV) of the jets, the collisional mean free paths of the jet ions are dominated by the physical mechanism of ions of one jet stopping on electrons of the other jet, i.e., a proper estimate is obtained via a test particle calculation with ion–electron collision rate given by  $\nu_s^{ie} \approx 1.6 \times 10^{-9} \mu^{-1} T_e^{-3/2} n_e Z^2 \ln \Lambda$  [45]. For nominal expected PLX argon jet parameters at  $R_m$  of  $v = 50$  km/s,  $n_e = 10^{16} \text{ cm}^{-3}$ , and  $T_e \sim 1$  eV, the collisional mean free path  $\sim v/\nu_s^{ie} = (50 \text{ km/s})/(1.83 \times 10^6 \text{ s}^{-1}) = 2.7 \text{ cm}$ , which is a nonnegligible fraction of the expected jet diameter at  $R_m$ .

2) *Liner Convergence*: After the jets merge to form an imploding spherical liner, the liner converges toward the center of the chamber. Both theoretical [18] and numerical modeling

[21] have shown that the liner density rises during the quasi-steady-state prestagnation phase of convergence as  $\rho \sim \rho_0 r^{-2}$ . However, as the liner approaches stagnation, different dynamics take over (discussed below in Section III-D). A key issue during the convergence phase is the degree of liner nonuniformity (inherited at  $R_m$  upon jet merging) and the evolution of this nonuniformity, the reason being that nonuniformity is expected to reduce the achievable peak pressure at stagnation and exacerbate any convergent instabilities that may arise.

Examples of the expected 1-D evolution of liner pressure  $P$ , density  $\rho$ , temperature  $T$ , and velocity  $v$  during convergence (albeit for a single species, noncomposite liner; detailed studies of composite liners are ongoing) are given in [21, Fig. 4]; it should be mentioned that these results are for an ideal gas EOS with  $\gamma = 5/3$ , and that refinements to  $P(r)$ ,  $\rho(r)$ , and  $T(r)$  are expected when better EOS models are applied (also the subject of ongoing research). The importance of these refinements is that they are expected to give a better prediction of the liner thermodynamic state just prior to stagnation, which in turn determines the peak pressure and temperature upon stagnation and ultimately the fusion yield.

The uniformity of the liner during convergence is being examined using 3-D SPHC simulations. Initial results [47], [48] are promising in the sense that the relatively substantial nonuniformity present upon jet merging at  $R_m$  gets “smeared” by the time the liner reaches stagnation. Fig. 3 shows 3-D SPHC simulation results comparing the evolution of an initially spherically symmetric liner with the evolution of a liner formed by the merging of 30 discrete plasma jets. It is seen that the initial nonuniformity of the discrete jet case gets mostly smeared out during convergence so as to resemble the initially symmetric liner case at stagnation. The peak pressure achieved in both cases is similar. This is a promising initial result suggesting that very stringent requirements on the initial liner uniformity may not be required.

Related to liner nonuniformity are convergent instabilities (e.g., Rayleigh–Taylor) and associated material mix within an imploding composite liner. Even if the gross liner uniformity is deemed relatively unimportant for achieving a given peak pressure, instabilities and instability-induced material mix, i.e., trailing colder pusher material mixing and advancing ahead of the leading hotter fuel material, could degrade the peak pressure and temperature of the fuel at liner stagnation and therefore the fusion yield. For the case of a liner imploding on vacuum, initial SPHC modeling [48] shows that there are only very short durations of Rayleigh–Taylor instability when the jets merge and then again when the central pressure peaks up and the liner has not yet begun to decelerate strongly. Further studies are needed for this case, and for the case with a preformed magnetized target, to determine if and how Rayleigh–Taylor and other convergent instabilities and associated mix affect the quality of the implosion.

### C. Liner Magnetization

Crucial to the plasma liner MIF concept (and all low  $\rho r$  MIF concepts) is fuel magnetization, which reduces thermal transport so that significant fusion burn is realized at modest

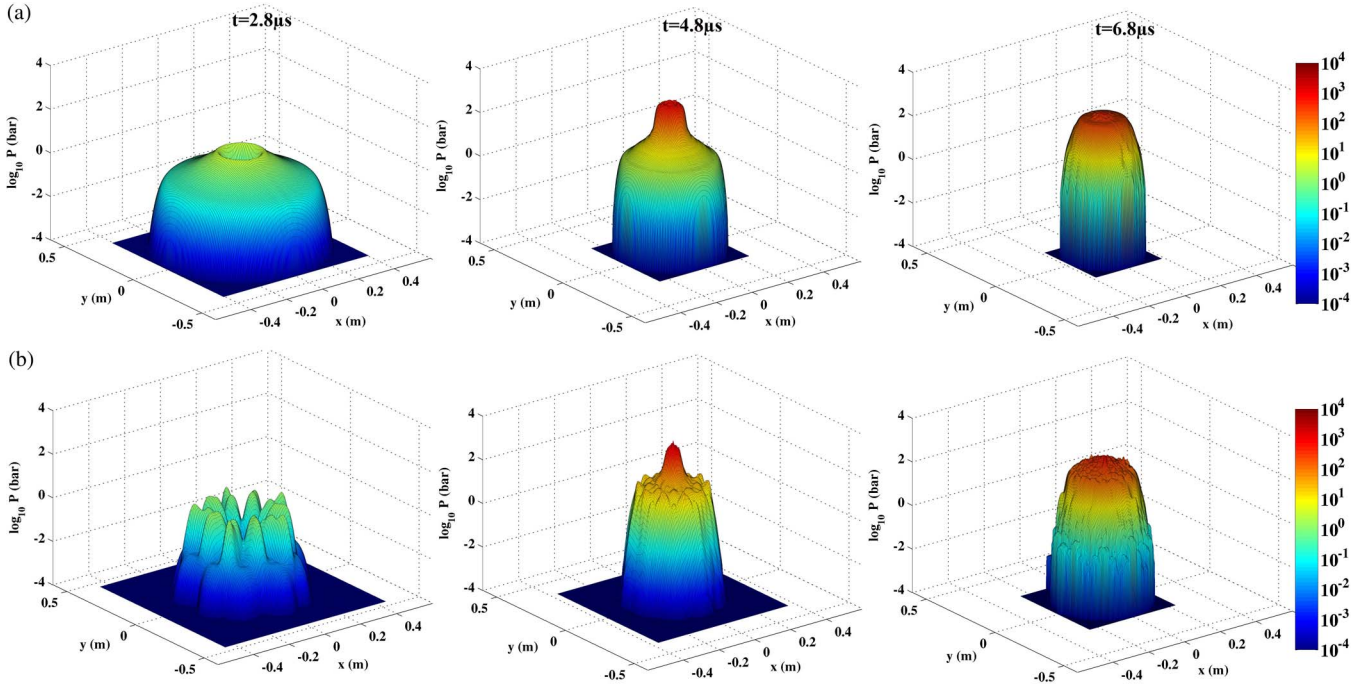


Fig. 3. Surface plots in the  $x-y$  plane of plasma liner pressure (logarithmic) from 3-D ideal hydrodynamic simulations. The top row shows the evolution of an initially spherically symmetric liner, and the bottom row shows the evolution of a liner formed from 30 discrete plasma jets.

implosion velocities of order 100 km/s or less. The required magnetic field magnitude in the fuel at peak compression is crudely determined by the condition  $\omega_{ci}\tau_i \gg 1$  (where  $\omega_{ci}$  and  $\tau_i$  are the ion gyro-frequency and collision time, respectively) such that particle heat transport is suppressed due to the magnetic field. For a representative compressed D-T fuel density of  $10^{21} \text{ cm}^{-3}$  and temperature of 10 keV, the condition becomes  $B \gg 7.1 \text{ T}$ . Because it is not known how to directly apply such a field within the compressed hot fuel, MIF concepts generally compress a more modest “seed” field of order 1 T to order 100 T by virtue of field compression that scales as the compression ratio squared, i.e.,  $B_f = B_i C^2 = B_i (r_i/r_f)^2$ , where for MTF concepts  $C \approx 10$ . For plasma liner MIF, the objective is to introduce the required seed magnetic field in the D-T fuel prior to peak compression such that the needed field strength is achieved at peak compression. The question of achieving a particular field topology is set aside for now and considered briefly later in this section.

At present, the favored liner magnetization scheme is based on the idea of using beat waves [49], [50] generated by lasers to drive electrical current, which has the substantial advantage of also being a standoff system that would avoid destruction with every shot. This technique relies on resonant acceleration of plasma electrons (and therefore current drive and introduction of magnetic field) by a beat wave generated by two electromagnetic waves separated by a correctly tuned frequency. This has been demonstrated in low density plasmas using microwaves [51]. For the case of plasma liner MIF, it is envisioned that the D-T fuel will have a density of order  $10^{17} - 10^{18} \text{ cm}^{-3}$  when it is about 5–10 cm away from the origin. This sets requirements on both the minimum central frequency of the two electromagnetic waves (for penetrating the plasma) and the difference frequency (so that the beat wave

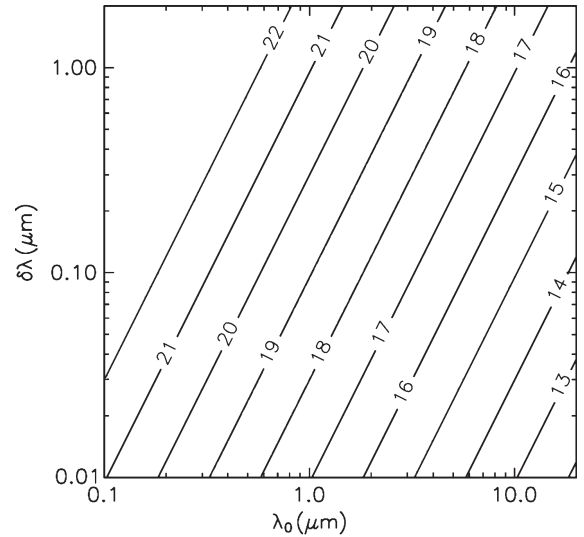


Fig. 4. Contours of the logarithm of the electron density (per cubic centimeter) as a function of the difference ( $\delta\lambda$ ) and central ( $\lambda_0$ ) wavelengths of the injected electromagnetic waves of frequency  $\omega_1$  and  $\omega_2$ , satisfying the beat wave resonance condition  $|\omega_1 - \omega_2| = \omega_{pe}$ .

is on the same order as the electron plasma frequency). Fig. 4 shows that electromagnetic waves with central wavelength  $\lambda_0 = (\lambda_1 + \lambda_2)/2 \sim 1 \mu\text{m}$  and a difference wavelength  $\delta\lambda = |\lambda_1 - \lambda_2| \sim 0.1 \mu\text{m}$  (e.g., Nd:YAG and/or Nd:YLF lasers) or  $\lambda_0 \sim 10 \mu\text{m}$  and  $\delta\lambda \sim 1 \mu\text{m}$  (e.g., CO<sub>2</sub> lasers) are needed. A recently initiated research project at University of California, Davis, has refurbished two CO<sub>2</sub> lasers for exploring the laser generated beat wave current drive technique, with estimated expected efficiency  $\sim 6 \times 10^{-7} \text{ A/W}$  and resultant  $\sim 60\text{-A}$  driven currents at 100 MW of laser power [52]. There is also a recently initiated coordinated PIC numerical modeling effort



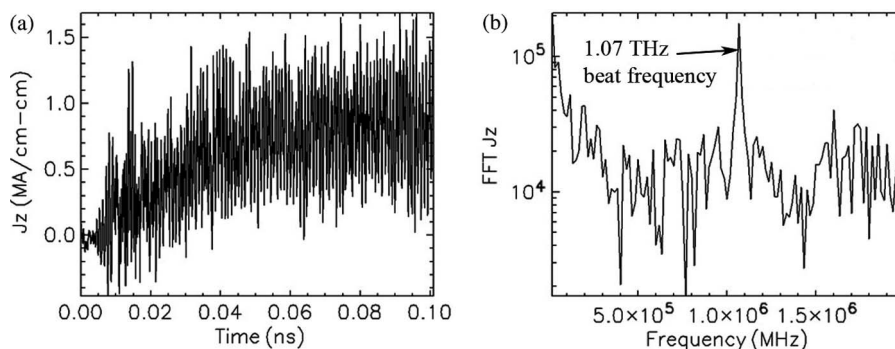


Fig. 5. LSP simulation result for counter-propagating laser beams of (left) growing current density versus time and (right) fast Fourier transform of the current density with a peak at the beat frequency.

of the beat wave generation and wave–particle interactions at PLX-relevant densities. The primary objectives of the modeling effort are to help optimize experiments on the beat wave generation and wave–particle coupling processes and to explore the important issue of current drive efficiency and how it scales up to plasma liner MIF relevant regimes. The simulations examined counter-propagating laser beam injection into a plasma with peak density of  $3 \times 10^{16} \text{ cm}^{-3}$ . Fig. 5 shows initial 2-D LSP collisional PIC simulation results confirming the growth of electrical current density and the presence of the beat wave near the expected 1.07-THz envelope frequency for injected beams at 10.4- and 10.8- $\mu\text{m}$  wavelengths and  $10^{13} \text{ W/cm}^2$  intensities (corresponding to available CO<sub>2</sub> lasers [52]). The electron acceleration proceeds in the direction of the higher frequency beam. In addition, the electron pressure exhibits strong axial modulation at the 5- $\mu\text{m}$  beat wave wavelength. Ongoing simulations are studying varying angles between injected laser beams and density gradients with the goal of optimizing the current drive with minimal heating.

The issue of field topology is an important one for plasma liner MIF. For the typically slower implosion MTF concepts, it is generally believed that closed flux surfaces in the preformed target are required to provide sufficient thermal insulation. It would be difficult (but not impossible, with some proprietary ideas being considered) to generate closed, mirror-like, or other flux surfaces via laser-generated beat wave current drive. However, a recent interesting work [53] suggests that a random field with sufficient connection length might provide sufficient thermal insulation for MIF, and this would open up the possibilities for fuel magnetization methodologies. Ongoing studies are evaluating different possible magnetic field topologies for plasma liner MIF that might be compatible with laser magnetization.

Another potential fuel magnetization scheme, perhaps a natural choice considering the conclusions in [53], would rely on compressing the initial magnetic fields embedded in the plasma jets themselves. However, this would be challenging because the magnitudes of the initially embedded magnetic fields are on the order of 0.1–1 T. At jet densities of  $\sim 10^{17} \text{ cm}^{-3}$  and temperatures of  $\sim 1 \text{ eV}$ , that field decays with an exponential time constant on the order of a few microseconds and thus would decrease to  $\ll 1 \text{ T}$  by the time the jets reached  $R_m$ . Understanding how the field would evolve and whether it would get amplified during subsequent convergence, and what field

topologies and structures are possible in the initial jet, would require further studies.

#### D. Stagnation and Disassembly

As the leading edge of the imploding liner reaches its minimum distance from the origin, it is compressed to high density and heated to high temperature, and stagnation is reached. An outgoing shock is formed and propagates outward into the incoming liner. This shock effectively converts the incoming liner kinetic energy into thermal energy of the postshocked stagnation region, which is the intended region for fusion burn (in the case of a composite liner with a D-T layer in the leading edge). The postshock region, after spiking to very high pressure, settles to a lower pressure and is maintained (within a factor of a few) until the outward propagating shock meets the back end of the incoming liner (see [21, Fig. 3]), at which time a rarefaction wave propagates inward quickly, leading to disassembly of the high pressure postshock region. The latter is qualitatively consistent with an analysis based on a self-similar model [54] and was anticipated in [8]. These dynamics are integral in determining the “dwell time” of the stagnated plasma and ultimately the fuel burn-up fraction, which is linearly proportional to the dwell time.

Recent theoretical work [55] based on a family of self-similar analytic solutions (so-called spherical quasi-simple waves) [56] to the spherically symmetric ideal hydrodynamic equations has led to the identification of an interesting potential method for optimizing the dwell time via specially chosen initial liner profiles of density and velocity, i.e., “shaped liners.” Such profiles admit an implosion solution (see Fig. 6) where the postshock high pressure region is maintained at constant pressure and zero velocity, with the region growing in size at a rate determined by the outgoing shock velocity. Physically, the outgoing shock converts the entire kinetic energy of the incoming liner into the thermal energy of the growing stagnated postshock region. Radiation-hydrodynamic numerical modeling is now proceeding to test these analytic solutions with finite liner thicknesses (the theory is exact only for infinite thickness liners), and eventually realistic effects such as thermal and radiation transport will be included to see if the solutions remain viable in realistic systems. Shaped liners, if they turn out to be viable, may be particularly well matched to the use of an afterburner D-T fuel layer because the outward shock could

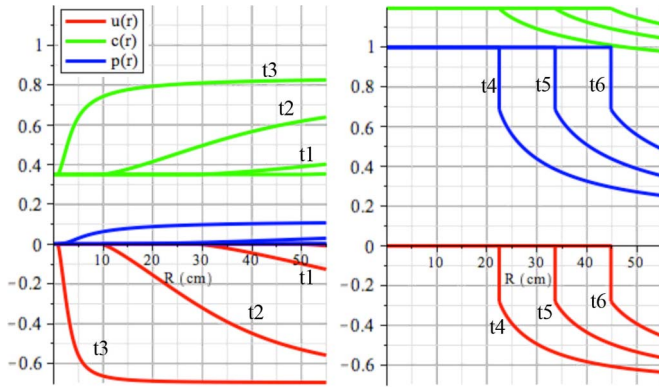


Fig. 6. Analytic solution for a self-similar imploding liner solution: normalized liner velocity  $u$ , sound speed  $c$ , and pressure  $p$  versus  $R$  for six successive times  $t_1$  through  $t_6$ . (Left) Liner converges toward origin. (Right) Stagnation shock propagates outward leaving a constant high pressure postshock region that grows in volume.

bring the afterburner layer up to the same (fusion-relevant) pressure of the inner compressed fuel. More studies are needed to investigate the feasibility of this scenario and whether any amplification of energy gain could be realized over the case without an afterburner layer.

#### E. Reactor Considerations

The plasma liner MIF concept was originally conceived [8] largely with the motivation of making an attractive fusion reactor by introducing a standoff driver embodiment to the otherwise attractive aspects of MIF. Such an embodiment eliminates repetitive destruction of materials such as solid liners and transmission lines and alleviates the “kopek problem” [57] of traditional MTF concepts, where the cost of the target package must be kept to a small fraction of the value of electricity that can be generated for each shot. Plasma liner MIF is also potentially amenable to other reactor-friendly technologies such as liquid plasma facing and tritium breeding technologies that would avoid a costly and time-consuming radiation-resistant materials development program. Power plant studies for MTF have been performed [57]–[59], and an initial reactor study of plasma liner MIF is in process [60]. The intention for plasma liner MIF is to aggressively pursue reactor-friendly technologies that are faster and cheaper to develop.

A key difference between plasma liner MIF and other MTF concepts is that the former, with its standoff driver, can in principle fire at higher repetition rates, e.g.,  $\sim 1$  Hz rather than  $\sim 0.1$  Hz. This would allow for lower energy yield per shot for the same average power, i.e.,  $\sim 100$  MJ rather than  $\sim 1$  GJ per shot for 100-MW average fusion power, which reduces thermal and radiative loading stresses on reactor components. For a 6-m diameter spherical first wall, this is a relatively modest  $0.9$  MW/m<sup>2</sup> of heat flux. On the other hand, the higher repetition rate places greater demands on pulsed power technology, including capacitor, plasma gun, and switch performance. The key issues are gun electrode erosion and pulsed power component lifetimes (at 1-Hz operation, this is  $3.15 \times 10^7$  shots/year). Clearly, much pulsed power research and development is needed to make pulsed power-based fusion

concepts, including plasma liner MIF, a reality. Solid-state switch technology is a promising choice for repetitive operation. Laser gated and pumped thyristor switches [61] developed for the KrF laser IFE program [62] have demonstrated ten million shot runs with small prototypes operating at 5 Hz while holding off 16.4 kV and switching 2.5 kA/cm<sup>2</sup> with  $dI/dt$  of 25 kA/ $\mu$ s/cm<sup>2</sup>. Repackaging into larger arrays to yield peak switched currents in the 200- to 300-kA (at least) range and increased voltage standoff would still need to be demonstrated.

Because the guns will likely be exposed to fusion neutrons and X-rays, they are deliberately chosen to be “low technology” and low cost in that they can potentially be made of radiation-resistant materials that are available today. The aim is to periodically replace the guns with minimal plant down time. Survivability of the jets themselves during the  $\sim 1$   $\mu$ s duration of the fusion blast will also require detailed assessment. The down time and shot repetition rate could be further reduced by operating several relatively low-cost imploding plasma liner fusion reactor cores (i.e., spherical chamber with plasma guns, standoff magnetization lasers, and liquid first wall) in parallel while sharing the same (more expensive) central tritium processing and electricity-generating balance-of-plant systems.

The hydrodynamic efficiency of a plasma liner (discussed in Section IV) is expected to be lower than that of a solid liner, and depending on how high of an energy gain is ultimately realizable, it may be necessary to implement technologies to recover part of the energy in the outgoing, poststagnation liner to keep the engineering gain as high as possible. Examples of potential liner energy recovery techniques were briefly discussed in [54] and would need further assessment for any plasma liner MIF reactor design. Additional studies are also needed to determine how much energy remains in the outgoing poststagnation liner (and how much is lost due to radiation).

Many of the reactor technologies envisioned for plasma liner MIF share commonalities with ICF reactors, particularly with heavy ion beam driven fusion, which has a substantial body of research, e.g., [63], from which to draw. In particular, flowing molten salts (such as FLiBe) as a plasma facing component and tritium breeding medium have been considered extensively for heavy ion fusion. The interesting technique of localized vortex liquid flows [64] on the inside surface of the vacuum chamber appears particularly well suited for plasma liner MIF, which requires gun penetrations distributed around the entire spherical chamber. Although the guns themselves would be sacrificial to neutron and hard X-ray damage (and would need periodic replacement), the spaces between guns would have localized vortex flows of a thick liquid molten salt that would protect the structure from neutrons and X-rays as well as breed tritium and serve as the coolant for driving the steam cycle to generate electricity. Adapting the vortex surface liquid flow method to plasma liner MIF and determining required flow rates and recirculating power are interesting and needed studies.

#### IV. SUMMARY OF 1-D IMPLoding SPHERICAL PLASMA LINER MODELING RESULTS

This section briefly summarizes the key results of recent 1-D radiation-hydrodynamic simulations [21] to study the PLX- and



MIF-relevant parameter space for imploding spherical plasma liners without a preformed magnetized target. Equivalent studies with a magnetized target are still needed. References to other PLX-relevant modeling efforts to date were provided in Section I and will not be discussed further here. The key results reported in [21] were 1) the qualitative evolution of an imploding spherical plasma liner, as described in Sections III-B2 and III-D; 2) that radiation and thermal transport must be included in simulations to avoid nonphysical extreme plasma temperatures at the origin, which artificially limit liner convergence and peak stagnation pressure; 3) a period  $\tau_{\text{stag}}$  of high postshock pressure is maintained according to  $\tau_{\text{stag}} \sim \Delta R_o / v_o$ , where  $\Delta R_o$  is the initial liner thickness, and  $v_o$  is the initial liner velocity; and 4) stagnation pressure  $P_{\text{stag}}$  (averaged over  $\tau_{\text{stag}}$ ) scales as  $v_o^{15/4}$ ,  $n_o^{1/2}$ , and  $M_o^{3/2}$  for a fixed initial liner geometry. The simulation results indicate that, for the case of 1-D spherically symmetric plasma liner implosion, a 376-kJ liner (achievable on PLX) can reach a maximum pressure of  $\sim 1.3$  Mbar with sustained pressure of  $\sim 0.1$  Mbar for over  $\sim 4 \mu\text{s}$  (run 6 of [21]). A more recent simulation, not contained in but adhering to the approach of [21], shows that a fusion-relevant pressure of  $\sim 50$  Mbar sustained for  $\sim 0.6 \mu\text{s}$  may be achieved with liner  $v_o \sim 150$  km/s and initial energy of 50 MJ. An important caveat is that these simulations are for targetless pure argon liners using an ideal gas EOS with (obviously) no fusion burn and no profile optimization. Further studies are needed to refine the velocity and liner energy requirements. As mentioned in Section III, initial 1-D ideal hydrodynamic studies [39] with a magnetized target and fusion burn suggest that implosion velocities  $< 50$  km/s and liner energy of 44 MJ could give energy gains of around 10. It is hoped to keep the implosion velocity  $< 100$  km/s to ease the requirements on the guns.

The liner hydrodynamic efficiency  $\eta$ , defined here as the maximum thermal energy of the poststagnated liner divided by the initial liner kinetic energy, is an important figure of merit for fusion systems and examined here using the argon (noncomposite) liner simulation results of [21]. Fig. 7(a) plots  $\eta$  and fusion figure of merit  $\eta P \tau$  versus initial liner velocity  $v_o$ . It is seen that  $\eta$  is low (only a few percent) for the cases run and decreases with  $v_o$ , but  $\eta P \tau$  (where  $P$  and  $\tau$  correspond to  $P_{\text{stag}}$  and  $\tau_{\text{stag}}$ , respectively, as previously defined) increases with  $v_o$ . The simulations also indicate that much of the initial liner kinetic energy is lost to radiation, and therefore, it will be critical to repeat this study with a D-T/Ar composite liner and better EOS/opacity modeling. Fig. 7(b) plots  $\tau_{\text{stag}}$ ,  $P_{\text{stag}}$ , the maximum stagnation region thermal energy  $E_{\text{max}}$ , and  $\eta$  versus  $\Delta R_o$ . Note that  $\eta$  is fairly insensitive to  $\Delta R_o$ . The reason is because the volume of high pressure, which itself is also rather insensitive to  $\Delta R_o$  and thus the total stagnated thermal energy, grows behind the outgoing shock until the shock reaches the back end of the incoming liner. From the simulation results (not shown here), it is seen that the maximum energy  $E_{\text{max}}$  occurs shortly before  $\tau_{\text{stag}}$ . Thus, a thicker liner allows for a higher  $E_{\text{max}}$ , as confirmed by Fig. 7(b). A thicker liner also keeps the interior stagnation pressure high for longer, thus extending  $\tau_{\text{stag}}$ . The finding that  $\eta$  is rather insensitive to  $\Delta R_o$  and the earlier finding that  $\tau_{\text{stag}} \sim \Delta R_o$  [21] both contradict [18].

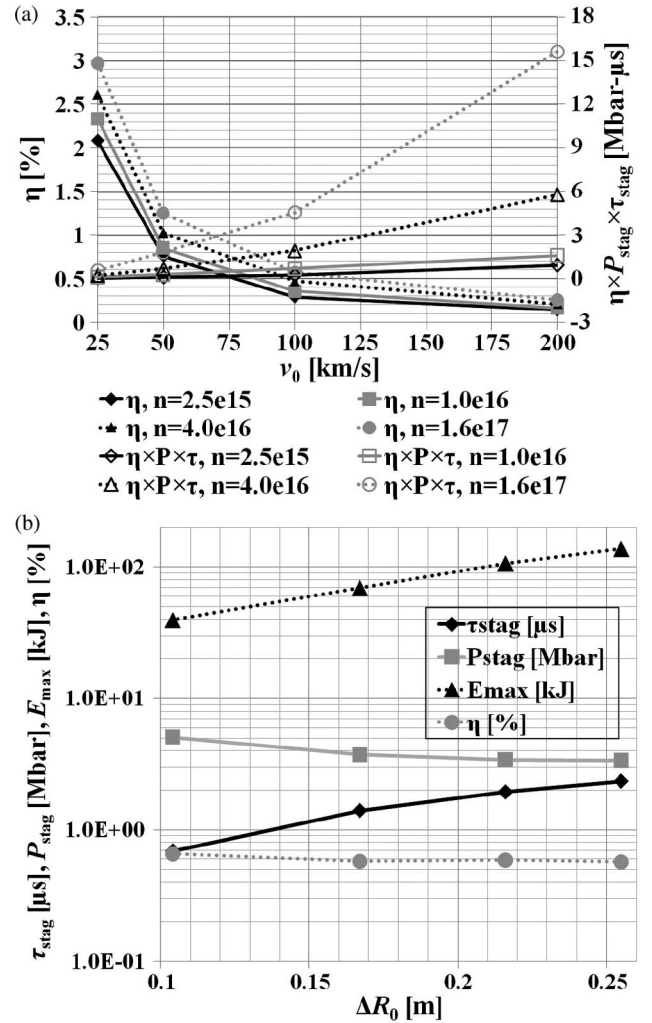


Fig. 7. (a) Liner efficiency  $\eta$  and fusion figure of merit  $\eta P \tau$  versus initial liner velocity  $v_o$  (data are from [21, Tab. II]). (b) Four parameters as indicated versus initial liner thickness  $\Delta R_o$  (data are from [21, Tab. III]).

## V. OVERVIEW OF THE PLX

As a first step toward evaluating the plasma liner MIF concept, the PLX at LANL is planning to explore and demonstrate the feasibility of forming imploding spherical plasma liners by merging an array of 30 high Mach number plasma jets [3]. A modest amount of pulsed power stored energy ( $\sim 1.5$  MJ) and kinetic energy of  $\sim 10$  kJ/jet, as planned, is sufficient to study the scientific issues associated with liner formation, convergence, and stagnation, while allowing access to centimeter-, microsecond-, and megabar-scale HED-relevant plasmas [21]. The latter enables a variety of fundamental studies of HED plasma science and laboratory plasma astrophysics, both near term objectives of PLX.

As of December, 2011, the PLX facility (see Fig. 8) has begun experimental operation focusing on physics studies of single-jet propagation and two-jet merging. The key scientific issues to be studied in phase one are 1) the expansion of the jet due to adiabatic and radiative cooling during propagation from the chamber wall to the merging radius  $R_m$ , and 2) the amount of interpenetration between two merging jets and the effects of shock formation (if any) on jet temperature and

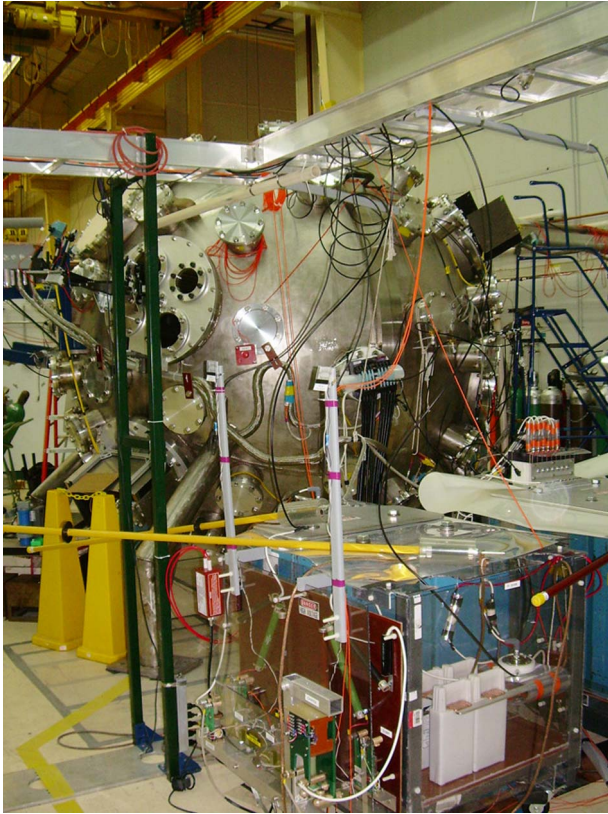


Fig. 8. Photograph of the PLX vacuum chamber (9' diameter) at LANL (Nov. 30, 2011), where single plasma jet experiments are underway. In the foreground are capacitor banks for the first two plasma guns.

compressibility. An eight-chord interferometer [65] is being used to measure the chord-averaged density at different jet propagation positions and the Abel-inverted density profiles in one plane of the jet transverse to the propagation direction. A visible and infrared spectroscopy system is being used in coordination with atomic physics modeling to evaluate the density and temperature evolution of the jet plasma as it propagates and expands. A laser-based Schlieren system that is sensitive to gradients in plasma density will be employed to image shock formation and evolution in the two-jet merging experiments. PLX diagnostics are described in more detail elsewhere [66]. Detailed diagnostic setup geometries have been utilized to generate synthetic interferometer and spectroscopy data based on LSP and Nautilus simulation results of single-jet propagation and two-jet merging. Comparisons with experimental data are underway.

Phase two of the experiment (planned for 2013, subject to available funding) will use 30 guns to investigate spherical plasma liner formation, convergence, and stagnation. Key scientific issues to be studied in phase two include the following: 1) peak pressure at stagnation as a function of initial jet parameters; 2) effects of liner nonuniformity on convergence and stagnation; and 3) stagnation and poststagnation liner dynamics. For the higher densities and temperatures expected in phase two, a vacuum ultraviolet spectroscopy system along with soft X-ray bolometry will be used to estimate the peak densities and temperatures of the stagnated liner [66].

## VI. SUMMARY

Plasma liner MIF is a standoff embodiment of MIF with many potentially attractive features for a fusion reactor. An updated concept-level description of plasma liner MIF is described in this paper. It is proposed to magnetize the D-T fuel just prior to peak compression via laser generated beat wave current drive, a technique that has been demonstrated experimentally at lower tokamak-relevant densities. Plasma liner MIF is intended to take advantage of many reactor-friendly features, including the use of a standoff driver to potentially increase shot repetition rate and improve cost-of-electricity economics as well as compatibility with integrated liquid first wall and tritium breeding approaches.

Theory and modeling efforts over the past few years have improved the understanding of the evolution of merging plasma jets and imploding plasma liners and have explored novel techniques such as the use of shaped liners to optimize the fusion-relevant performance of imploding plasma liners. These efforts have focused attention on key open scientific issues to be ultimately resolved by experiment, such as the beneficial radiative cooling of jets resulting in an increase rather than decrease in Mach number during jet propagation, the details of shock formation (if any) during jet merging and whether there is any substantial heating and Mach number downshift, liner uniformity, and material mix during convergence that could potentially degrade the peak pressure and temperature at stagnation, and the poststagnation dynamics of an imploded plasma liner that determine the confinement time and, ultimately, the fusion performance of a plasma liner MIF system. State-of-the-art 3-D radiation-MHD simulations of a full plasma liner MIF implosion are still needed for the best possible predictions of achievable fusion energy gain and for refining the concept.

The PLX at LANL plans to explore and demonstrate the feasibility of forming an imploding plasma liner via the merging of 30 plasma jets in spherically convergent geometry. As of December 2011, PLX has begun experimental operation, with initial campaigns focusing on scientific issues relating to single-jet propagation and two-jet merging. Subsequently, starting in 2013, 30 jet experiments on PLX will focus on studying liner formation, convergence, and stagnation with expected peak pressures of 1 Mbar sustained for order  $1 \mu\text{s}$ . In the near term, PLX will enable a unique scientific platform for fundamental studies of spherically imploded HED plasmas by generating centimeter-, microsecond-, and megabar-scale plasmas, and in the longer term, it could provide a platform to further explore and develop the plasma liner MIF concept.

## ACKNOWLEDGMENT

The authors would like to thank Dr. Y. C. F. Thio for encouragement, extensive discussions, and sharing initial 1-D hydrodynamic simulation results on fusion energy gain for the plasma liner MIF concept. The authors would also like to thank all their collaborators at LANL, HyperV Technologies, University of Alabama in Huntsville, University of New Mexico, FAR-TECH, Voss Scientific, Prism Computational Sciences, Tech-X, University of California, Davis, and University of Chicago.



## REFERENCES

- [1] I. R. Lindemuth and R. C. Kirkpatrick, "Parameter space for magnetized fuel targets in inertial confinement fusion," *Nucl. Fusion*, vol. 23, no. 3, pp. 263–284, Mar. 1983.
- [2] R. C. Kirkpatrick, I. R. Lindemuth, and M. S. Ward, "Magnetized target fusion: An overview," *Fusion Technol.*, vol. 27, pp. 201–214, 1995.
- [3] S. C. Hsu, F. D. Witherspoon, J. T. Cassibry, and M. A. Gilmore, "Overview of the plasma liner experiment," in *Proc. Bull. Amer. Phys. Soc.*, 2011, vol. 56, p. 307.
- [4] I. R. Lindemuth, R. E. Reinovsky, R. E. Chrien, J. M. Christian, C. A. Ekdahl, J. H. Goforth, R. C. Haight, G. Idzorek, N. S. King, R. C. Kirkpatrick, R. E. Larson, G. L. Morgan, B. W. Olinger, H. Oona, P. T. Sheehy, J. S. Shlachter, R. C. Smith, L. R. Veaser, B. J. Warthen, S. M. Younger, V. K. Chernyshev, V. N. Mokhov, A. N. Demin, Y. N. Dolin, S. F. Garanin, V. A. Ivanov, V. P. Korchagin, O. D. Mikhailov, I. V. Morozov, S. V. Pak, E. S. Pavlovskii, N. Y. Seleznev, A. N. Skobelev, G. I. Volkov, and V. A. Yakubov, "Target plasma formation for magnetic compression/magnetized target fusion," *Phys. Rev. Lett.*, vol. 75, no. 10, pp. 1953–1956, Sep. 1995.
- [5] T. Intrator, S. Y. Zhang, J. H. Degnan, I. Furno, C. Grabowski, S. C. Hsu, E. L. Ruden, P. G. Sanchez, J. M. Taccetti, M. Tuszewski, W. J. Waganar, and G. A. Wurden, "A high density field reversed configuration (FRC) target for magnetized target fusion: First internal profile measurements of a high density FRC," *Phys. Plasmas*, vol. 11, no. 5, pp. 2580–2585, May 2004.
- [6] M. Labege, "Experimental results for an acoustic driver for MTF," *J. Fusion Energy*, vol. 28, no. 2, pp. 179–182, Jun. 2009.
- [7] G. Votroubek and J. Slough, "The plasma liner compression experiment," *J. Fusion Energy*, vol. 29, no. 6, pp. 571–576, Dec. 2010.
- [8] Y. C. F. Thio, E. Panarella, R. C. Kirkpatrick, C. E. Knapp, F. Wysocki, P. Parks, and G. Schmidt, "Magnetized target fusion in a spheroidal geometry with standoff drivers," in *Proc. 2nd Int. Symp.—Current Trends International Fusion Research*, E. Panarella, Ed., 1999, p. 113.
- [9] Y. C. F. Thio, C. E. Knapp, R. C. Kirkpatrick, R. E. Siemon, and P. J. Turchi, "A physics exploratory experiment on plasma liner formation," *J. Fusion Energy*, vol. 20, no. 1/2, pp. 1–11, Jun. 2001.
- [10] C. E. Knapp, "An implicit smooth particle hydrodynamic code," Ph.D. dissertation, Univ. New Mexico, Albuquerque, NM, 2000.
- [11] Y. C. F. Thio, J. T. Cassibry, and T. E. Markusic, "Pulsed electromagnetic acceleration of plasmas," presented at the 38th AIAA/ASME/SAE/ASEE Joint Propulsion Conf. Exhibit, Indianapolis, IN, Jul. 7–10, 2002, Paper AIAA-2002-3803.
- [12] J. T. Cassibry, Y. C. F. Thio, and S. T. Wu, "Two-dimensional axisymmetric magnetohydrodynamic analysis of blow-by in a coaxial plasma accelerator," *Phys. Plasmas*, vol. 13, no. 5, pp. 053101-1–053101-13, May 2006.
- [13] F. D. Witherspoon, S. Brockington, A. Case, S. J. Messer, L. Wu, R. Elton, S. C. Hsu, J. T. Cassibry, and M. A. Gilmore, "Development of minirailguns for the plasma liner experiment," in *Proc. Bull. Amer. Phys. Soc.*, 2011, vol. 56, p. 311.
- [14] F. D. Witherspoon, A. Case, S. J. Messer, R. Bomgardner, jr., M. W. Phillips, S. Brockington, and R. Elton, "A contoured gap coaxial plasma gun with injected plasma armature," *Rev. Sci. Instrum.*, vol. 80, no. 8, p. 083506, Aug. 2009.
- [15] A. Case, S. Messer, R. Bomgardner, and F. D. Witherspoon, "Interferometer density measurements of a high-velocity plasmoid," *Phys. Plasmas*, vol. 17, no. 5, p. 053503, May 2010.
- [16] W. Liu and S. C. Hsu, "Ideal magnetohydrodynamic simulations of unmagnetized dense plasma jet injection into a hot strongly magnetized plasma," *Nucl. Fusion*, vol. 51, no. 7, p. 073026, Jul. 2011.
- [17] S. C. Hsu, "Technical summary of the first U.S. plasma jet workshop," *J. Fusion Energy*, vol. 28, no. 3, pp. 246–257, Sep. 2009.
- [18] P. B. Parks, "On the efficacy of imploding plasma liners for magnetized fusion target compression," *Phys. Plasmas*, vol. 15, no. 6, p. 062506, Jun. 2008.
- [19] D. R. Welch, D. V. Rose, M. E. Cuneo, R. B. Campbell, and T. A. Mehlhorn, "Integrated simulation of the generation and transport of proton beams from laser-target interaction," *Phys. Plasmas*, vol. 13, no. 6, p. 063105, Jun. 2006.
- [20] [Online]. Available: <http://www.prism-cs.com>
- [21] T. J. Awe, C. S. Adams, J. S. Davis, D. S. Hanna, S. C. Hsu, and J. T. Cassibry, "One-dimensional radiation-hydrodynamic scaling studies of imploding spherical plasma liners," *Phys. Plasmas*, vol. 18, no. 7, p. 072705, Jul. 2011.
- [22] R. J. Kanzleiter, W. L. Atchison, R. L. Bowers, R. L. Fortson, J. A. Guzik, R. T. Olson, J. L. Stokes, and P. J. Turchi, "Using pulsed power for hydrodynamic code validation," *IEEE Trans. Plasma Sci.*, vol. 30, no. 5, pp. 1755–1763, Oct. 2002.
- [23] J. J. Monaghan, "Smoothed particle hydrodynamics," *Ann. Rev. Astron. Astrophys.*, vol. 30, pp. 543–574, Sep. 1992.
- [24] C. A. Wingate and R. F. Stellingwerf, "Smooth particle hydrodynamics—The sphynx and SPHC codes," Los Alamos Nat. Lab., Los Alamos, NM, Tech. Rep. LA-UR-93-1938, 1993.
- [25] J. T. Cassibry, M. D. Stanic, T. J. Awe, D. S. Hanna, J. S. Davis, S. C. Hsu, and F. D. Witherspoon, "Theory and modeling of the plasma liner experiment," in *Proc. Bull. Amer. Phys. Soc.*, 2010, vol. 55, p. 359.
- [26] C. Thoma, D. R. Welch, R. E. Clark, N. Bruner, J. J. MacFarlane, and I. E. Golovkin, "Two-fluid electromagnetic simulations of plasma-jet acceleration with detailed equation-of-state," *Phys. Plasmas*, vol. 18, no. 10, p. 103507, Oct. 2011.
- [27] J. Loverich and A. Hakim, "Two-dimensional modeling of ideal merging plasma jets," *J. Fusion Energy*, vol. 29, no. 6, pp. 532–539, Dec. 2010.
- [28] R. P. Drake, "The design of laboratory experiments to produce collisionless shocks of cosmic relevance," *Phys. Plasmas*, vol. 7, no. 77, pp. 4690–4698, Nov. 2000.
- [29] "Basic research needs for high energy density laboratory physics—Report of the DOE Workshop on HEDLP Research Needs," U.S. Dept. Energy, Washington, DC, Nov. 15–18, 2009.
- [30] M. M. Basko, A. J. Kemp, and J. M. ter Vehn, "Ignition conditions for magnetized target fusion in cylindrical geometry," *Nucl. Fusion*, vol. 40, no. 1, pp. 59–68, Jan. 2000.
- [31] R. H. Lovberg and C. L. Daily, "Large inductive thruster performance measurement," *AIAA J.*, vol. 20, no. 7, pp. 971–977, Jul. 1982.
- [32] D. E. Johnson and D. P. Bauer, "The effect of rail resistance on railgun efficiency," *IEEE Trans. Magn.*, vol. 25, no. 1, pp. 271–276, Jan. 1989.
- [33] I. R. Lindemuth and R. E. Siemon, "The fundamental parameter space of controlled thermonuclear fusion," *Amer. J. Phys.*, vol. 77, no. 5, pp. 407–416, May 2009.
- [34] S. A. Slutz, M. C. Herrmann, R. A. Vesey, A. B. Sefkow, D. B. Sinars, D. C. Rovang, K. J. Peterson, and M. E. Cuneo, "Pulsed-power-driven cylindrical liner implosions of laser preheated fuel magnetized with an axial field," *Phys. Plasmas*, vol. 17, no. 5, p. 056303, May 2010.
- [35] P. Y. Chang, P. Y. Chang, G. Fiksel, M. Hohenberger, J. P. Knauer, R. Betti, F. J. Marshall, D. D. Meyerhofer, F. H. Séguin, and R. D. Petrasso, "Fusion yield enhancement in magnetized laser-driven implosions," *Phys. Rev. Lett.*, vol. 107, no. 3, pp. 035006-1–035006-4, Jul. 2011.
- [36] J. Slough, S. Andreason, H. Gota, C. Pihl, and G. Votroubek, "The pulsed high density experiment: Concept, design, and initial results," *J. Fusion Energy*, vol. 26, no. 1/2, pp. 199–205, Jun. 2007.
- [37] A. Y. Chirkov and S. V. Ryzhkov, "The plasma jet/laser driven compression of compact plasmoids to fusion conditions," *J. Fusion Energy*, vol. 31, no. 1, pp. 7–12, Feb. 2012.
- [38] S. F. Garanin, "The MAGO system," *IEEE Trans. Plasma Sci.*, vol. 26, no. 4, pp. 1230–1238, Aug. 1998.
- [39] Y. C. F. Thio, private communication, 2011.
- [40] M. M. Marinak, R. E. Tipton, O. L. Landen, T. J. Murphy, P. Amendt, S. W. Haan, S. P. Hatchett, C. J. Keane, R. McEachern, and R. Wallace, "Three-dimensional simulations of NOVA high growth factor capsule implosion experiments," *Phys. Plasmas*, vol. 3, no. 5, pp. 2070–2076, May 1996.
- [41] A. Ciardi, S. V. Lebedev, A. Frank, E. G. Blackman, J. P. Chittenden, C. J. Jennings, D. J. Ampleford, S. N. Bland, S. C. Bott, J. Rapley, G. N. Hall, F. A. Suzuki-Vidal, A. Marocchino, T. Lery, and C. Stehle, "The evolution of magnetic tower jets in the laboratory," *Phys. Plasmas*, vol. 14, no. 5, pp. 056501-1–056501-10, May 2007.
- [42] P. J. Turchi, N. F. Roderick, J. H. Degnan, M. H. Frese, and D. J. Amdahl, "Review of plasma gun techniques for fusion at megagauss energy densities," *IEEE Trans. Plasma Sci.*, vol. 38, no. 8, pp. 1864–1873, Aug. 2010.
- [43] J. R. Thompson, N. I. Bogatu, S. A. Galkin, J. S. Kim, D. R. Welch, C. Thoma, J. J. MacFarlane, F. D. Witherspoon, J. T. Cassibry, T. J. Awe, and S. C. Hsu, "Plasma jet propagation and stability modeling for the plasma liner experiment," in *Proc. Bull. Amer. Phys. Soc.*, 2010, vol. 55, p. 360.
- [44] C. Thoma, private communication, 2011.
- [45] J. D. Huba, NRL Plasma Formulary, 2009.
- [46] R. Samulyak, P. Parks, and L. Wu, "Spherically symmetric simulation of plasma liner driven magnetoinertial fusion," *Phys. Plasmas*, vol. 17, no. 9, p. 092702, Sep. 2010.
- [47] J. T. Cassibry, M. Stanic, R. Hatcher, S. Hsu, D. Witherspoon, M. Gilmore, and W. Luo, "The tendency of plasma liners formed by hypersonic jets to



- evolve toward good spherical symmetry during implosion,” in *Proc. Bull. Amer. Phys. Soc.*, 2011, vol. 56, p. 311.
- [48] J. T. Cassibry, M. Stanic, S. C. Hsu, S. I. Abarzhi, and F. D. Witherspoon, “Tendency of spherically imploding plasmas liners formed by merging plasma jets to evolve toward spherical symmetry,” submitted for publication.
- [49] M. N. Rosenbluth and C. S. Liu, “Excitation of plasma waves by two laser beams,” *Phys. Rev. Lett.*, vol. 29, no. 11, pp. 701–705, Sep. 1972.
- [50] A. N. Kaufman and B. I. Cohen, “Nonlinear interaction of electromagnetic waves in a plasma density gradient,” *Phys. Rev. Lett.*, vol. 30, no. 26, pp. 1306–1309, Jun. 1973.
- [51] J. H. Rogers and D. Q. Hwang, “Measurements of beat-wave-accelerated electrons in a toroidal plasma,” *Phys. Rev. Lett.*, vol. 68, no. 26, pp. 3877–3880, Jun. 1992.
- [52] F. Liu, R. Horton, D. Q. Hwang, R. Evans, Z. F. Huang, and A. Semet, “Laser-driven beat-wave current drive in an unmagnetized plasma,” presented at the 38th European Physical Society Conf. Plasma Physics, Strasbourg, France, 2011, paper P2.023.
- [53] D. D. Ryutov, “Adiabatic compression of a dense plasma ‘mixed’ with random magnetic fields,” *Fus. Sci. Tech.*, vol. 56, no. 4, pp. 1489–1494, Nov. 2009.
- [54] J. T. Cassibry, R. J. Cortez, S. C. Hsu, and F. D. Witherspoon, “Estimates of confinement time and energy gain for plasma liner driven magnetoinertial fusion using an analytic self-similar converging shock model,” *Phys. Plasmas*, vol. 16, no. 11, p. 112707, Nov. 2009.
- [55] G. Kagan, X. Tang, S. C. Hsu, and T. J. Awe, “Bounce-free spherical hydrodynamic implosion,” *Phys. Plasmas*, vol. 18, no. 12, p. 120702, Dec. 2011.
- [56] R. Courant and K. O. Friedrichs, *Supersonic Flow and Shock Waves*. Berlin, Germany: Springer-Verlag, 1976.
- [57] R. L. Miller, “Perspectives on magnetized target fusion power plants,” *J. Fusion Energy*, vol. 26, no. 1/2, pp. 119–121, Jun. 2007.
- [58] R. W. Moses, R. A. Krakowski, and R. L. Miller, “A conceptual design of the fast-liner reactor (FLR) for fusion power,” Los Alamos Nat. Lab., Los Alamos, NM, Tech. Rep. LA-7686-MS, 1979.
- [59] R. L. Miller, “Liner-driven pulsed magnetized target fusion power plant,” *Fusion Sci. Technol.*, vol. 52, no. 3, pp. 427–431, Oct. 2007.
- [60] R. L. Miller, private communication, 2011.
- [61] D. Weidenheimer, D. Morton, G. James, D. Giorgi, T. Navapanich, D. Knudsen, and R. Knight, “Scaled-up LGPT (laser gated and pumped thyristor) devices at KrF IFE (inertial fusion energy) operating parameters,” in *Conf. Rec. 27th Int. Power Modulator Symp.*, 2006, pp. 201–206.
- [62] J. D. Sethian, M. Friedman, J. L. Giuliani, R. H. Lehberg, S. P. Obenschain, P. Kepple, M. Wolford, F. Hegeler, S. B. Swanekamp, D. Weidenheimer, D. Welch, D. V. Rose, and S. Searles, “Electron beam pumped KrF lasers for fusion energy,” *Phys. Plasmas*, vol. 10, no. 5, pp. 2142–2146, May 2003.
- [63] R. W. Moir, “The high-yield lithium-injection fusion-energy (HYLIFE)-II inertial fusion energy (IFE) power plant concept and implications for IFE,” *Phys. Plasmas*, vol. 2, no. 6, pp. 2447–2452, Jun. 1995.
- [64] P. M. Bardet, B. F. Supiot, P. F. Peterson, and O. Savas, “Liquid vortex shielding for fusion energy applications,” *Fusion Sci. Technol.*, vol. 47, no. 4, pp. 1192–1196, May 2005.
- [65] E. C. Merritt, A. G. Lynn, M. A. Gilmore, and S. C. Hsu, “Multi-chord fiber-coupled interferometer with a long coherence length laser,” *Rev. Sci. Instrum.*, accepted for publication, 2012.
- [66] A. G. Lynn, E. Merritt, M. Gilmore, S. C. Hsu, F. D. Witherspoon, and J. T. Cassibry, “Diagnostics for the plasma liner experiment,” *Rev. Sci. Instrum.*, vol. 81, no. 10, p. 10E115, Oct. 2010.
- S. C. Hsu**, photograph and biography not available at the time of publication.
- T. J. Awe**, photograph and biography not available at the time of publication.
- S. Brockington**, photograph and biography not available at the time of publication.
- A. Case**, photograph and biography not available at the time of publication.
- J. T. Cassibry**, photograph and biography not available at the time of publication.
- G. Kagan**, photograph and biography not available at the time of publication.
- S. J. Messer**, photograph and biography not available at the time of publication.
- M. Stanic**, photograph and biography not available at the time of publication.
- X. Tang**, photograph and biography not available at the time of publication.
- D. R. Welch**, photograph and biography not available at the time of publication.
- F. D. Witherspoon**, photograph and biography not available at the time of publication.